PHYSICAL REVIEW E VOLUME 50, NUMBER 2 AUGUST 1994

Viscoelasticity of concentrated dispersions

T. S. Chow
Xerox Webster Research Center, 800 Phillips Road, 0114-39D, Webster, New York 14580

(Received 7 April 1994)

A statistical dynamic theory is presented to describe the effects of relaxation of the microstructure, frequency, and volume fraction (ϕ) on the complex shear viscosity of concentrated colloidal dispersions. On the basis of a fluid lattice model, the relationship between the memory function and relaxation spectrum is derived, and the limits of shear viscosity at low and high frequencies are determined. In addition to the pair interactions, the many body interactions at higher ϕ are included in the analysis. We calculate the viscoelastic behavior of disperse systems ranging from dilute, to semidilute, to concentrated dispersions. The theory reveals that the viscoelastic effect is negligible in dilute and semidilute suspensions, but is dominant in concentrated dispersions.

PACS number(s): 82.70.Dd, 05.20.−y, 61.25.Hq, 82.70.Kj

I. INTRODUCTION

Stable colloidal dispersions often exhibit clear viscoelastic behavior [1,2]. The structural relaxation of the microstructure and its response to shear flow are the key to understanding and controlling the phenomenon. The linear viscoelasticity is manifested in the frequency dependent dynamic viscosity. The viscosity of dilute suspensions is independent of frequency. As the concentration of colloidal particles increases, the viscosity becomes frequency dependent [3,4]. For semidilute suspensions, theories for the frequency dependent shear viscosity [5–9] have been developed. They are either phenomenological or pair interaction theories, which can be used to calculate the dynamic viscosity to second order in the volume fraction (ϕ) of colloidal particles. Cichocki and Felderhof have also discussed the viscoelastic relaxation of semidilute hard-sphere suspensions over decades of frequency variations in their phenomenological theory [5,6]. Experimental data of Van der Werff *et al.* [2] have shown that the viscoelasticity is particularly important for dense suspensions with ϕ between 0.3 and 0.6. This viscoelastic effect increases drastically when ϕ approaches the percolation threshold [10]. Therefore, it is important to have a theory which can explain the complex shear viscosities at higher volume fractions ($\phi > 0.3$). No such theory is available at the present time, and it is the purpose of this paper to develop one.

Much of the diversity in the viscoelasticity of colloidal dispersions can be seen clearly through an integral equation for simple shear flow in Sec. II. The key to understanding the complex viscosity lies in analyzing the structural relaxation of the microstructure. The relaxation time spectrum and memory function are derived in Sec. III and then applied to calculate master curves of the dynamic viscosity in Sec. IV. Our analysis is based on statistical mechanics, expressed in terms of a liquid lattice model. The limits of viscosity at low and high frequencies are given in Sec. V. At the low frequency limit, we analyze the many body interactions of colloidal particles moving in a liquid lattice. Finally, a microscopic theory is obtained to describe the complex shear viscosity of sterically stabilized colloidal dispersions as a function of the relaxation time, frequency, and volume fraction. The theory is utilized to predict the viscoelastic behavior of disperse systems ranging from dilute, to semidilute, to concentrated dispersions.

II. VISCOELASTICITY

The linear constitutive equation of the shear stress (σ_{12}) and strain rate ($\dot{\gamma}_{12}$) for a viscoelastic liquid can be written by means of the Boltzmann superposition integral [11]

$$\sigma_{12}(t)=\int_{-\infty}^{t} G(t-s)\dot{\gamma}_{12}(s)ds \ , \tag{1}$$

where G is the shear relaxation modulus and t is time. When Eq. (1) is subjected to the Fourier transform in time

$$\sigma_{12}[\omega]=\int_{-\infty}^{t} \sigma_{12}(t)\exp(-i\omega t)dt \ , \tag{2}$$

it can be written in the form

$$\frac{\sigma_{12}[\omega]}{\gamma_{12}[\omega]}=G(\omega)=i\omega\int_{0}^{\infty} G(t)\exp(-i\omega t)dt \ , \tag{3}$$

where ω is the angular frequency. The complex shear viscosity $\eta(\omega)$ can be related to the complex modulus by

$$\eta(\omega)=\eta'-i\eta''=\frac{\sigma_{12}[\omega]}{\dot{\gamma}_{12}[\omega]}=\frac{G(\omega)}{i\omega}=\frac{G'+iG''}{i\omega} \ . \tag{4}$$

Hence

$$\eta'(\omega)=G''(\omega)/\omega, \quad \eta''(\omega)=G'(\omega)/\omega \ . \tag{5}$$

The complex modulus can in general be written as

$$G(\omega)=G_{\infty}+(G_0-G_{\infty})K(\omega) \ , \tag{6}$$

where K is the relaxation function, G_0 is the unrelaxed modulus, and G_{∞} is the relaxed modulus. In the similar fashion, we have

1063-651X/94/50(2)/1274(6)/$06.00

$$\eta(\omega)=\eta_\infty+(\eta_0-\eta_\infty)M(\omega)\ , \tag{7}$$

where η_0 and η_∞ are the limits of viscosity at low and high frequencies and M is the memory function. Equations (6) and (7) give

$$M(t)=-\tau\frac{dK(t)}{dt}\ , \tag{8}$$

where τ is the relaxation time. It is the ratio of the low-frequency viscosity over the modulus of rigidity: $\tau=\eta_0/G_0$. In the rest of the paper, we shall analyze $\eta(\omega)$ as a function of the solvent viscosity η_2, ϕ, ω, and τ.

III. MEMORY FUNCTION

The Maxwell model of viscoelasticity gives the simplest relaxation function

$$K_{\text{Maxwell}}(t)=\exp\left[-\frac{t}{\tau}\right]\ . \tag{9}$$

For a real system, Eq. (9) has to be generalized

$$K(t)=\sum_i h_i\exp\left[-\frac{t}{\tau_i}\right]\ , \tag{10}$$

where h_i and τ_i are the distribution and relaxation time, respectively, of the ith relaxation element. By letting

$$\tau_i/\tau\rightarrow s,\quad h_i\rightarrow h(s)\ , \tag{11}$$

the summation in Eq. (10) can be written as an integral

$$K(t/\tau)=\int_0^\infty h(s)\exp(-st/\tau)ds\ , \tag{12}$$

where $h(s)$ is called the relaxation time spectrum. When the distribution is a delta function $h(s)=\delta(s-1)$, Eq. (12) reduces to Eq. (9) as expected. From Eqs. (6), (7), and (12), one gets

$$M(t/\tau)=\int_0^\infty sh(s)\exp(-st/\tau)ds\ . \tag{13}$$

On the basis of the free volume or hole theories of the liquid state [12,13], a liquid lattice model [10] has been developed recently and it provides a good description of colloidal dynamics at high ϕ. Lattice models are basically theories of solid state and have the advantage of providing good connections between the dense liquid and amorphous solid [14,15]. Consider a lattice consisting of n holes (free volumes) in a disperse system and n is much less than the total number of lattice sites (N). The hole configurations change with time in response to shear flow. We introduce the local excess of number density $\delta n(\mathbf{r},t)$, where $\mathbf{r}$ is the spatial variable. Then

$$n(t)-\langle n\rangle=\int\delta n(\mathbf{r},t)d\mathbf{r}\ , \tag{14}$$

where $\langle n\rangle$ is the equilibrium value and the integration is taken over a volume element surrounding a hole. The hole density-density correlation function is

$$C(\mathbf{r},t)=\frac{\langle\delta n(\mathbf{r},t)\delta n(0,0)\rangle}{\langle\delta n^2\rangle}\ . \tag{15}$$

The local excess of number density relaxes as time goes on by spreading over the entire medium in accordance with the master equation [14]

$$\frac{\partial\delta n(\mathbf{r},t)}{\partial t}=\int[\Lambda(\mathbf{r}|\mathbf{r}')\delta n(\mathbf{r}',t)-\Lambda(\mathbf{r}'|\mathbf{r})\delta n(\mathbf{r},t)]d\mathbf{r}'\ , \tag{16}$$

where $\Lambda(\mathbf{r}|\mathbf{r}')$ is the transition probability per unit time jumping from $\mathbf{r}'$ to $\mathbf{r}$ and the integration is over the whole space. The right-hand side of Eq. (16) can be formally expanded into a series [16]. Thus

$$\frac{\partial\delta n(\mathbf{r},t)}{\partial t}=\sum_{m=1}^\infty\frac{1}{m!}(-\nabla)^m b_m(\mathbf{r})\delta n(\mathbf{r},t)\ , \tag{17}$$

where b_m is the mth moment of the transition rate $\Lambda(\mathbf{r}|\mathbf{r}')$

$$b_m(\mathbf{r})=\int(\mathbf{r}'-\mathbf{r})^m\Lambda(\mathbf{r}'|\mathbf{r})d\mathbf{r}',\quad m\geq 1\ . \tag{18}$$

Since the viscoelasticity of concentrated dispersions is a result of relaxation of the microstructure in quasiequilibrium, the right-hand side of Eq. (17) is truncated after the second order term. Equations (15) and (17) give

$$\left[\frac{\partial}{\partial t}-\nabla\cdot\frac{b_2}{2}\nabla\right]C(\mathbf{r},t)=\delta(\mathbf{r})\delta(t)\ . \tag{19}$$

When $b_2/2$ is a (diffusion) constant, the solution of Eq. (19) is Gaussian

$$C(\mathbf{r},t)=\frac{1}{(2\pi b_2 t)^{1/2}}\exp\left[-\frac{x^2}{2b_2 t}\right]\ . \tag{20}$$

By considering the structural relaxation in a fixed length scale, the relaxation spectrum can be related to the hole density-density correlation function [15]. We choose $x=1$ and $b_2t/2=s$, replace $C(s)/s$ by $h(s)$ in Eq. (20), and obtain

$$h(s)=\frac{1}{2(\pi s^3)^{1/2}}\exp\left[\frac{1}{4s}\right]\ . \tag{21}$$

Substituting Eq. (21) into Eqs. (12) and (13) gives, respectively, the relaxation function

$$K(t/\tau)=\exp[-(t/\tau)^{1/2}] \tag{22}$$

and the memory function

$$M(t/\tau)=\tfrac{1}{2}(\tau/t)^{1/2}\exp[-(t/\tau)^{1/2}]\ . \tag{23}$$

IV. COMPLEX VISCOSITY

The dynamic shear viscosity $\eta(\omega)$ is related to the memory function by Eq. (7)

$$\frac{\eta(\omega)-\eta_\infty}{\eta_0-\eta_\infty}=M(\omega\tau)=\int_0^\infty M(y)\exp(-i\omega\tau y)dy\ . \tag{24}$$

Substituting Eq. (23) into Eq. (24), we obtain

$$\frac{\eta(\omega)-\eta_\infty}{\eta_0-\eta_\infty}=\frac{\pi^{1/2}}{2(\omega\tau)^{1/2}}\exp\left[\frac{1}{4(\omega\tau)^{1/2}}\right]\operatorname{erfc}\left[\frac{1}{2(\omega\tau)^{1/2}}\right]$$
$$=\frac{1}{2}\left[\frac{\pi}{2\omega\tau}\right]^{1/2}(1-i)W\left[\frac{1+i}{2(2\omega\tau)^{1/2}}\right], \tag{25}$$

where [17]

$$W\left[\frac{1+i}{2(2\omega\tau)^{1/2}}\right]=\exp\left[\frac{1}{4\omega\tau}\right]\left[1+\frac{2i}{(\pi)^{1/2}}\int_0^{(1+i)2(2\omega\tau)^{-1/2}}e^{-z^2}dz\right]. \tag{26}$$

The real and imaginary parts of the complex shear viscosity can be written explicitly by expressing Eq. (25) in terms of the Fresnel integrals

$$C\equiv C[(2\pi\omega\tau)^{-1/2}]=\int_0^{(2\pi\omega\tau)^{-1/2}}\cos\left[\frac{\pi}{2}z^2\right]dz \tag{27}$$

and

$$S\equiv S[(2\pi\omega\tau)^{-1/2}]=\int_0^{(2\pi\omega\tau)^{-1/2}}\sin\left[\frac{\pi}{2}z^2\right]dz\ . \tag{28}$$

Therefore

$$\frac{\eta'(\omega)-\eta_\infty}{\eta_0-\eta_\infty}=\frac{1}{2}\left[\frac{\pi}{2\omega\tau}\right]^{1/2}\left[(1-2S)\cos\left[\frac{1}{4\omega\tau}\right]-(1-2C)\sin\left[\frac{1}{4\omega\tau}\right]\right] \tag{29}$$

and

$$\frac{\eta''(\omega)}{\eta_0-\eta_\infty}=\frac{1}{2}\left[\frac{\pi}{2\omega\tau}\right]^{1/2}\left[(1-2C)\cos\left[\frac{1}{4\omega\tau}\right]+(1-2S)\sin\left[\frac{1}{4\omega\tau}\right]\right]. \tag{30}$$

The dependence of η' and η'' on $\omega\tau$, calculated from Eqs. (29) and (30), is shown in Fig. 1, which compares well with the normalized viscosities shown in Fig. 9 of Ref. [2]. The maximum value of the calculated $\eta''(\omega)/(\eta_0-\eta_\infty)$ is very close to the corresponding measured value 0.3 for all volume fractions. The relaxation time τ is also found to be linear proportional to a^2/D. Here D is the Stokes-Einstein diffusion coefficient $D=kT/6\pi\eta_2\,a$, a is the particle radius, and η_2 is the solvent viscosity. This is another indication of the strong coupling between the relaxation of the shear stress and that of the microstructure.

For large $\omega\tau$, the asymptotic expression of the complex shear viscosity can be obtained from Eq. (25), which gives

$$\frac{\eta'(\omega)-\eta_\infty}{\eta_0-\eta_\infty}\simeq 0.627(\omega\tau)^{-1/2},\quad \text{for } \omega\tau\gg 1 \tag{31}$$

and

$$\frac{\eta''(\omega)}{\eta_0-\eta_\infty}\simeq 0.627(\omega\tau)^{-1/2}\quad \text{for } \omega\tau\gg 1\ . \tag{32}$$

Both η' and η'' decay as $\omega^{-1/2}$. Equations (29) and (31) are compared in Fig. 2. This figure supports the experimental finding [2] of the high-frequency scaling law Eq. (31): it also provides a good description of the dynamic viscoelastic data at the intermediate-frequency range for all particle concentrations. Next we need to know η_0 and η_∞ before the effect of volume fractions on the dynamic viscosity can be calculated.

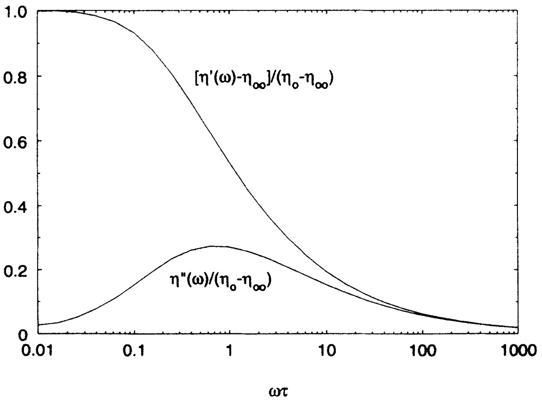

FIG. 1. Calculated master curves of the real and imaginary part of the complex shear viscosity as a function of $\omega\tau$ for all ϕ.

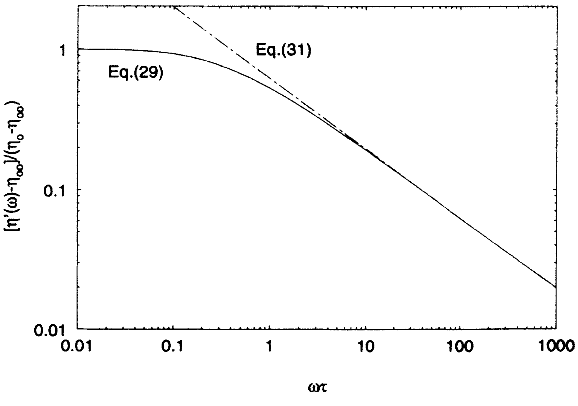

FIG. 2. A comparison of Eq. (29) with its asymptote given by Eq. (31) over a broad range of $\omega\tau$ for all ϕ.

V. LIMITS OF VISCOSITY

The viscosity of colloidal suspensions at the high-frequency limit has been derived on the basis of a liquid lattice model [10]. The short range intermolecular interaction within the equilibrium microstructure is the dominant interaction mechanism at high ϕ. For a system dispersed with hard spheres, the relative high shear limiting viscosity is

$$\eta_r(\infty)\equiv\frac{\eta_\infty}{\eta_2}=\exp\left[\frac{2.5\phi}{1-\phi}\right] . \tag{33}$$

The difference between low and high limiting viscosities $\Delta\eta$ is a result of the energy being dissipated per unit time and volume, which is related to the decrease in the kinetic energy (K_E):

$$\Delta\eta\equiv\eta_0-\eta_\infty=\langle d(K_E)/dt\rangle/\dot{\gamma}_{12}^2 . \tag{34}$$

For particles moving in an inverse-square force field, the classical result $\langle K_E\rangle=-\frac{1}{2}\langle P_E\rangle$ (where P_E denotes potential energy) holds. When the contribution of all the two-particle interactions in a disperse system is included, Eq. (34) becomes [18]

$$\Delta\eta_r=\left\langle -\frac{1}{2}\sum_{i>j} r_{ij}\frac{\partial V(r_{ij})}{\partial r_{ij}}\right\rangle , \tag{35}$$

where V is the nondimensional pair potential and r_{ij} is the distance between centers of two spheres. The summation in Eq. (35) is over all pair interactions. The right-hand side of Eq. (35) can be written into an integral

$$-\int\int \rho(r_{12})r_{12}\frac{\partial V(r_{12})}{\partial r_{12}}d\mathbf{r}_1 d\mathbf{r}_2 , \tag{36}$$

where ρ is the pair distribution function.

The potential energy between two colloidal particles arising from the intermolecular interaction energy (ε), which characterizes the equilibrium microstructure on the basis of our hole theory of liquid lattice [10], is

$$u(X)=\begin{cases}-\varepsilon/f & \text{for } X<1\\ 0 & \text{for } X\geq 1 ,\end{cases} \tag{37}$$

with $X=r/2a$, where $f=n/N$ is the hole fraction. The equilibrium radial distribution function follows:

$$g_0(X)=\exp\left[-\frac{u(X)}{kT}\right]=\begin{cases}v\equiv\exp(+\varepsilon/fkT)\\ \quad\text{for } X<1\\ 1 \quad \text{for } X\geq 1 .\end{cases} \tag{38}$$

For incompressible fluids, one approximates $\rho\sim g_0\psi$, where ψ is determined by the Kirkwood-Smoluchowski equation [5,19]

$$\frac{d}{dX}\left[X^2 g_0\frac{d\psi}{dX}\right]-6g_0\psi=4X^3\frac{dg_0}{dX} . \tag{39}$$

Therefore, Eqs. (35) and (36) can be expressed more explicitly as

$$\Delta\eta_r=-\frac{9\phi^2}{5}\int_0^\infty X^3\frac{dV(x)}{dX}g_0(X)\psi(X)dX\equiv A\phi^2 , \tag{40}$$

where A is the coupling constant. Noting $V=g_0$ in thermodynamic equilibrium, we use Eq. (38) and get

$$\frac{dV(X)}{dX}=\frac{g_0(X)}{dX}=-(v-1)\delta(X-1) . \tag{41}$$

The boundary conditions for Eq. (39) are that ψ vanishes at infinity and the requirement that the pair distribution function is a continuous function. There is no discontinuity at $X=1$. The solution of Eq. (39) is [19]

$$\psi(X)=\begin{cases}\alpha X^2 & \text{for } X\leq 1\\ \alpha/X^3 & \text{for } X>1\end{cases} \tag{42}$$

with $\alpha=4(v-1)/(2v+3)$. Substituting Eqs. (38), (41), and (42) into Eq. (40) yields

$$A=\tfrac{9}{5}(v-1)\int_0^\infty X^3 g_0\psi(X)\delta(X-1)dX=\frac{36(v-1)^2}{5(2v+3)} . \tag{43}$$

Equations (40) and (43), derived with the basic elements of pair interaction theories [1,5,6], should be valid only for semidilute suspensions.

As ϕ gets higher, the effective viscosity has to be affected by the strong many body interactions. Consider the probability $P(2,1)$ of a colloidal particle moving from point 1 to point 2 in a dense dispersion. This probability is the sum of the probabilities of all the different ways that the colloidal particle may propagate from 1 to 2. Of course, it interacts with various local lattice sites on its path. For simplicity, we consider only one kind of local site which has the probability $P(s)$. The total probability is

$$P(2,1)=P_0(2,1)+P_0(s,1)P(s)P_0(2,s)$$
$$+P_0(s,1)P(s)P_0(s,s)P(s)P_0(2,s)+\cdots . \tag{44}$$

The first term $P_0(2,1)$ is the probability of free propagation without the interference from the local site. In the second term, $P_0(s,1)$ is the probability of the colloidal particle which can propagate freely from 1 to site s and $P_0(2,s)$ from s to 2. The third term can be interpreted in the same way. This idea of the propagation of a particle is due to Feynman, and Eq. (44) can be represented by the Feynman diagram [20]

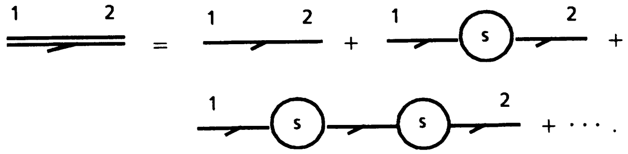

(45)

From the diagram we can immediately write down all the various contributions to P, and the interpretation is straightforward. $P_0(2,1)$ has a Boltzmann-type probability distribution [18]

$$P_0(2,1)=1-\exp(-E_0/kT)\simeq E_0/kT ,$$
$$\text{for } E_0/kT\ll 1 , \tag{46}$$

where k is Boltzmann's constant. Since $P_0(2,1)$ is essentially describing the case of two particle interaction, E_0 can be treated as the pair potential and is related to the nondimensional coupling constant in Eq. (40) by

$$E_0 \Longrightarrow A\phi^2 \ . \tag{47}$$

Assume the total probability $P(2,1)$ having the same functional form of Eq. (46) and

$$P_0(2,1)=P_0(s,1)=P_0(2,s)=P_0(s,s) \ . \tag{48}$$

From Eqs. (40), (44), (47), and (48), we obtain

$$\Delta\eta_r = A\phi^2\{1+[A\phi^2P(S)]+[A\phi^2P(S)]^2 + [A\phi^2P(S)]^3+\cdots\} \ . \tag{49}$$

Combining Eqs. (33) and (49) yields the low limiting viscosity

$$\eta_r(0)=\eta_r(\infty)+\Delta\eta_r=\exp\left[\frac{2.5\phi}{1-\phi}\right]+\frac{A\phi^2}{1-A\phi^2P(s)} \ , \tag{50}$$

which also leads to the percolation threshold at the low-frequency limit

$$\phi_c=[A(\varepsilon/f)P(s)]^{-1/2} \ , \tag{51}$$

where A is given by Eq. (43) and is a strong function of ε/f. There is a drastic increase in the effective relative viscosity $\eta_r(0)$ as $\phi\to\phi_c$. $P(s)$ may be either treated as a fitting parameter of experimental data or calculated in accordance with our liquid lattice model by specifying the structural detail. The many body interaction during the passage of colloidal particle is analyzed with a set of fixed lattice sites. $P(s)$ is the probability of the particle being "scattered" and $1-P(s)$ being able to go through. Thus $P(s)$ is equal to the maximum packing fraction of the unit structural volume filled with "spheres." Assuming the body centered cubic lattice, we have $P(s)=0.68$. Since the random process for holes discussed in Sec. III is Gaussian, this results in $\varepsilon/f=1.25kT$ for stable dispersions [10]. Hence the coupling constant $A=4.67$ from Eq. (43). Figure 3 shows the comparison between the theory Eqs. (33) and (50) and experimental data [3,4] for polystyrene latices in water and for silica spheres in cyclohexane at high- and low-frequency limits ranging from dilute, to semidilute, to concentrated dispersions. This theory also reveals that the disperse systems have a more "ordered" structure at low frequency than that at the high frequency.

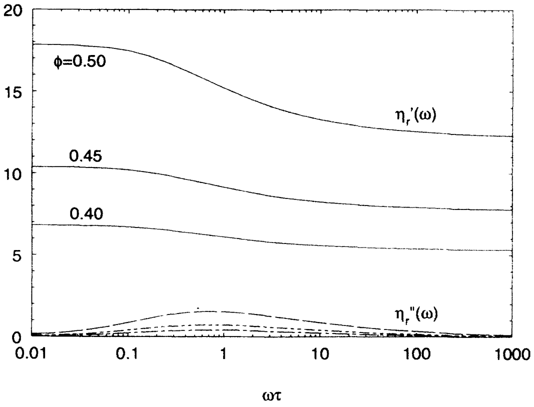

FIG. 4. Calculated real and imaginary part of the relative complex shear viscosity over the full frequency range and with ϕ from 0.40 to 0.50.

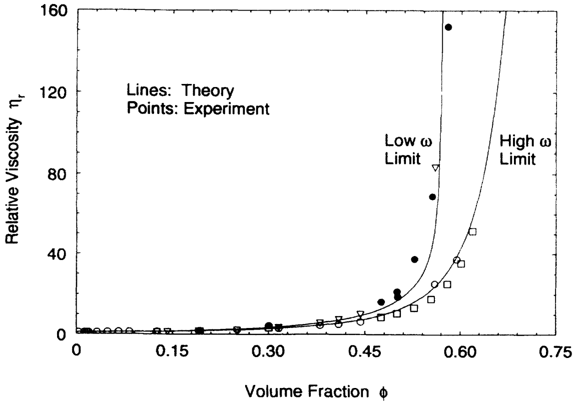

FIG. 3. Calculated low and high limiting viscosities [from Eqs. (33) and (50)] compared with the experimental data [3,4] for polystyrene latices in water and silica spheres in cyclohexane.

Finally, we are in the position to calculate the real and imaginary part of the relative complex shear viscosity over the full ranges of volume fraction and frequency by using Eqs. (29), (30, (33), and (50), with the coupling constant A and probability $P(s)$ already mentioned. The calculated results are shown in Figs. 4 and 5. The lower parts of these two figures $[\eta_r''(\omega)\equiv\eta''(\omega)/\eta_2]$ correspond to the upper parts $[\eta_r'(\omega)\equiv\eta'(\omega)/\eta_2]$. The highest curve of $\eta_r''(\omega)$ corresponds to the highest volume fraction in each figure. Figures 3–5 reveal that the viscoelasticity of stable colloidal dispersions becomes important for $\phi>0.3$. The viscoelastic effect increases rapidly as $\phi\to\phi_c$, which is consistent with experimental measurements [2].

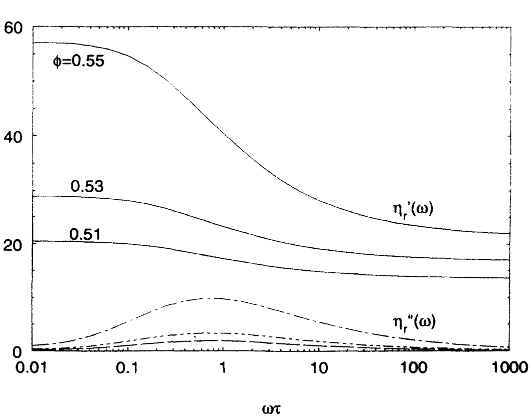

FIG. 5. Calculated real and imaginary part of the relative complex shear viscosity over the full frequency range and with ϕ from 0.51 to 0.55.

VI. CONCLUSIONS

A liquid lattice model has been developed to address the relaxation of the microstructure and the viscoelastic response in colloidal dispersions as a function of the relaxation time, frequency, and volume fraction. The good agreement between the calculated and measured master curves of the complex shear viscosity suggests that the structural relaxation in disperse systems is independent of the volume fraction of hard spheres (ϕ). The high-frequency scaling law with $\omega^{-1/2}$ decay for the complex viscosity has also been found to be valid in the intermediate-frequency range for all ϕ. In addition to the structural relaxation, the limits of viscosity at low and high frequencies are needed in the calculation of the dependence of the dynamic viscosity on ϕ. As the concentration of colloidal particles increases, we have to include the many body interaction between the colloidal particle and fluid lattice in the evaluation of the low limit viscosity. Our theory reveals that the viscoelasticity of stable disperse systems is important only for $\phi > 0.3$. The viscoelastic effect increases drastically as ϕ approaches a critical value ϕ_c. This percolation threshold is inversely proportional to the square root of the coupling constant which is related to the strength of intermolecular interactions.

[1] W. B. Russel, D. A. Saville, and W. R. Schowalter, *Colloidal Dispersions* (Cambridge University Press, Cambridge, 1989).

[2] J. C. Van der Werff, C. G. de Kruif, C. Blom, and J. Mellema, Phys. Rev. A **39**, 795 (1989).

[3] I. M. Krieger, Adv. Colloid Interface Sci. **3**, 111 (1972).

[4] C. G. de Kruif, E. M. F. van Iersel, A. Vrij, and W. B. Russel, J. Chem. Phys. **83**, 4717 (1985).

[5] B. Cichocki and B. U. Felderhof, Phys. Rev. A **46**, 7723 (1992).

[6] B. Cichocki and B. U. Felderhof, Phys. Rev. A **43**, 5405 (1991).

[7] J. Blawzdziewicz and G. Szamel, Phys. Rev. E **48**, 4632 (1993).

[8] E. G. D. Cohen and I. M. de Schepper, J. Stat. Phys. **63**, 241 (1991).

[9] C. W. J. Beenakker, Physica A **128**, 48 (1984).

[10] T. S. Chow, Phys. Rev. E **48**, 1977 (1993).

[11] J. D. Ferry, *Viscoelastic Properties of Polymers*, 3rd ed. (Wiley, New York, 1980).

[12] T. H. Hill, *Statistical Mechanics* (Dover, New York, 1987), Chap. 8.

[13] A. K. Doolittle, J. Appl. Phys. **22**, 1471 (1951).

[14] T. S. Chow, Phys. Rev. A **44**, 6916 (1991).

[15] T. S. Chow, Adv. Polym. Sci. **103**, 149 (1992).

[16] J. E. Moyal, J. R. Stat. Soc. B **11**, 150 (1949).

[17] *Handbook of Mathematical Functions*, Natl. Bur. Stand. Appl. Math. Ser. No. 55, edited by M. Abramowitz and I. A. Stegun (U.S. GPO, Washington, DC, 1964).

[18] R. P. Feynman, *Statistical Mechanics* (Benjamin, Reading, MA, 1972).

[19] J. G. Kirkwood, F. P. Buff, and M. S. Green, J. Chem. Phys. **17**, 988 (1949).

[20] G. Rickayzen, *Green's Functions and Condensed Matter* (Academic, New York, 1980).